2005

Surface and Bulk Transitions in Three-Dimensional O(n) Models

Youjin Deng

Henk W.J. Blöte

See next page for additional authors

Citation/Publisher Attribution

Deng, Y., Blöte, H. W.J., & Nightingale, M. P. (2005). Surface and bulk transitions in three-dimensional O(n) models. *Physical Review E*, 72(1), 016128. doi: 10.1103/PhysRevE.72.016128
Available at: http://dx.doi.org/10.1103/PhysRevE.72.016128

Surface and bulk transitions in three-dimensional O(n) models

Youjin Deng,[1,2] Henk W. J. Blöte,[2,3] and M. P. Nightingale[4]
[1]*Laboratory for Materials Science, Delft University of Technology, Rotterdamseweg 137, 2628 AL Delft, The Netherlands*
[2]*Faculty of Applied Sciences, Delft University of Technology, P.O. Box 5046, 2600 GA Delft, The Netherlands*
[3]*Lorentz Institute, Leiden University, P.O. Box 9506, 2300 RA Leiden, The Netherlands*
[4]*Department of Physics, University of Rhode Island, Kingston, Rhode Island 02881, USA*
(Received 16 March 2005; published 27 July 2005)

Using Monte Carlo methods and finite-size scaling, we investigate surface criticality in the O(n) models on the simple-cubic lattice with $n=1$, 2, and 3, i.e., the Ising, XY, and Heisenberg models. For the critical couplings we find $K_c(n=2)=0.454\,1659\ (10)$ and $K_c(n=3)=0.693\,003\ (2)$. We simulate the three models with open surfaces and determine the surface magnetic exponents at the ordinary transition to be $y_{h1}^{(o)}=0.7374\ (15)$, 0.781 (2), and 0.813 (2) for $n=1$, 2, and 3, respectively. Then we vary the surface coupling K_1 and locate the so-called special transition at $\kappa_c(n=1)=0.502\,14\ (8)$ and $\kappa_c(n=2)=0.6222\ (3)$, where $\kappa=K_1/K-1$. The corresponding surface thermal and magnetic exponents are $y_{t1}^{(s)}=0.715\ (1)$ and $y_{h1}^{(s)}=1.636\ (1)$ for the Ising model, and $y_{t1}^{(s)}=0.608\ (4)$ and $y_{h1}^{(s)}=1.675\ (1)$ for the XY model. Finite-size corrections with an exponent close to $-1/2$ occur for both models. Also for the Heisenberg model we find substantial evidence for the existence of a special surface transition.

DOI: 10.1103/PhysRevE.72.016128 PACS number(s): 05.50.+q, 64.60.Cn, 64.60.Fr, 75.10.Hk

I. INTRODUCTION

In the past decades, surface effects near a phase transition have been investigated extensively, and many results have been obtained by means of the mean-field theory, series expansions, renormalization, and field-theoretic analyses. For reviews, see, e.g., Refs. [1,2], and for more recent work see Refs. [3,4]. In particular, at a second-order phase transition, where long-range correlations emerge, surface effects can be significant. The surfaces display critical phenomena which differ from the bulk critical behavior; several surface universality classes can exist for one bulk universality class. We shall refer to the various types of transitions using the terminology of Ref. [1].

In this work, we investigate surface critical phenomena in three-dimensional O(n) models, namely the Ising ($n=1$), the XY ($n=2$), and the Heisenberg ($n=3$) model. The reduced Hamiltonian of these models can be written as the sum of two parts: a bulk term proportional to the volume of the system and a surface term proportional to the surface area, i.e.,

$$\mathcal{H}/k_BT = -K\sum_{\langle ij\rangle} {}^{(b)}\vec{s}_i\cdot\vec{s}_j - \vec{H}\cdot\sum_k {}^{(b)}\vec{s}_k - K_1\sum_{\langle pq\rangle} {}^{(s)}\vec{s}_p\cdot\vec{s}_q - \vec{H}_1\cdot\sum_r {}^{(s)}\vec{s}_r, \quad (1)$$

where the dynamic variable $\vec{s}$ is a unit vector of n components. The parameters K and K_1 are the strengths of the coupling between nearest-neighbor sites in the bulk and on the surface layers, respectively, and H and H_1 represent the reduced magnetic fields. The first two sums in Eq. (1) account for the bulk and the last two sums involve the spins on the open surfaces. For ferromagnetic bulk and surface couplings ($K>0$ and $K_1>0$), the phase transitions are sketched in Fig. 1 for the case of the Ising and the XY model. In the high-temperature region, i.e., for bulk coupling $K<K_c$, the bulk is in the paramagnetic state, so that the bulk correlation length remains finite. However, a phase transition can still occur on the open surface when the surface coupling K_1 is sufficiently enhanced. This phase transition is referred to as the "surface transition," and is represented by the solid curve in Fig. 1. These phase transitions are generally thought to be in the same universality classes as the two-dimensional Ising and the XY model, respectively. At the bulk critical point $K=K_c$, the line of surface phase transitions terminates at a point (K_c,K_{1c}). At this point, both the surface and the bulk correlation length diverge. Thus, the point (K_c,K_{1c}) acts as a multicritical point, and the phase transition is referred to as the "special transition." For $K_1<K_{1c}$, the bulk and the surfaces simultaneously undergo a phase transition at $K=K_c$. In this case, the critical correlations on the surfaces arise from the

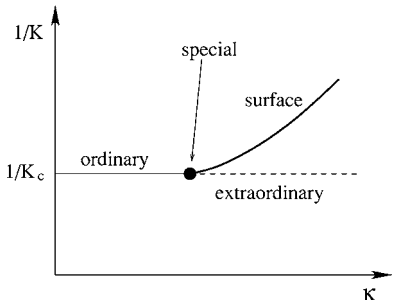

FIG. 1. Sketch of the surface phase transitions of the three-dimensional Ising and XY models with ferromagnetic couplings. The vertical axis is the bulk temperature $1/K$, and the parameter $\kappa=(K_1-K)/K$ in the horizontal axis represents the enhancement of the surface couplings. The "surface," the "ordinary," and the "extraordinary" phase transitions are represented by the thick solid, the thin solid, and the dashed line, respectively. The lines meet in a point, shown as the black circle, which is referred to as the "special" phase transition.

diverging bulk correlation lengths, and the transition is named the "ordinary transition." The ordinary transition remains within the same universality class for a wide range of surface couplings. The correlation functions on and near the surface appear to fit universal profiles [5]. The transitions at $K=K_c$ for $K_1>K_{1c}$ are referred to as the "extraordinary transitions." For the Ising model, since the surfaces are already in the ferromagnetic state for a smaller coupling $K<K_c$, no surface transition occurs when the bulk critical line $K=K_c$ is crossed. Nevertheless, owing to the diverging bulk correlation length, the surfaces still display critical correlations at $K=K_c$. For the *XY* model, however, the surface transitions for $K<K_c$ are Kosterlitz–Thouless-like [6], i.e., the surfaces do not display long-range order for $K<K_c$, in agreement with results of Landau and co-workers [7].

For three-dimensional O(n) models with $n>2$, which include the Heisenberg model, the line of surface transitions for $K<K_c$ does not exist; it may thus seem self-evident that the special and the extraordinary transitions are also absent. However, this remains to be investigated; for instance, in two-dimensional tricritical Potts models, a line of edge transitions is absent, but special and extraordinary transitions do exist [8]. Thus, even without a line of surface transitions for $K<K_c$, rich surface critical phenomena can still occur in the three-dimensional Heisenberg model. For instance, it was reported [9] that at bulk criticality $K=K_c$ the surface magnetic exponents depend on the ratio K_1/K for $K_1/K \geqslant 2.0$. This brings up the question whether one can locate a true phase transition as a function of K_1/K.

Additional surface critical phenomena can occur for the Ising model, if the surface and/or the bulk couplings are allowed to be antiferromagnetic. Further, one can allow the spins on the surface to vanish, such that the surface part of the Hamiltonian in Eq. (1) is described by the so-called Blume–Capel model. Such spin-0 states act as annealed vacancies on the surfaces. It was observed [10] that, by varying the fugacity of the vacancies, one can reach a point where the bulk Ising criticality $K=K_c$ joins the line of surface transitions that belongs to the universality class of the two-dimensional tricritical Ising model. This point was named [10] the "tricritical special" phase transition. In short, for each bulk universality class, surface transitions in various surface universality classes can occur, including the ordinary, special, and extraordinary transitions at $K=K_c$, and the surface transitions at $K<K_c$.

Apart from the bulk renormalization exponents, additional surface exponents are needed to describe the above surface critical behavior. At the ordinary and the extraordinary transitions, the surface magnetic scaling field is relevant, while the surface thermal field is irrelevant. At the special transition, both the magnetic and the thermal surface fields are relevant.

Since exact information about critical behavior is scarce in three dimensions, determinations of these surface critical exponents rely on approximations of various kinds. These include the mean-field theory [1,11–13], series expansions [14], renormalization group technique [2,3,15–17], Monte Carlo simulations [5,7,18–22], etc.

The surface critical index β_1 is defined so as to describe the asymptotic scaling behavior of the surface magnetization m_1 as a function of the bulk thermal field t, i.e., $m_1 \propto t^{\beta_1}$. From the scaling relations it follows that this exponent is related to the critical exponents as $\beta_1=(d-1-y_{h1})/y_t$, where y_t and y_{h1} are the bulk thermal and the surface magnetic exponent, respectively, and $d=3$ is the spatial dimensionality. The mean-field analysis and the Gaussian fixed point of the ϕ^4 theory yield the magnetic surface index β_1 as $\beta_1^{(o)}=1$, $\beta_1^{(s)}=1/2$, and $\beta_1^{(e)}=1$, respectively, for the ordinary, special, and extraordinary transition. Many numerical results also exist. For the simple-cubic lattice, the special transition of the Ising model was located as $\kappa_c=0.5004$ (2) [19,20]. Although the values of critical couplings K_c and K_{1c} are far from the mean-field predictions, the above result for κ_c is in agreement with the mean-field value $\kappa_c=1/2$. Further, the surface critical exponents are determined [19–21,23] as $y_{h1}^{(o)}=0.737$ (5), $y_{h1}^{(s)}=1.62$ (2), and $y_{t1}^{(s)}=0.94$ (6). Compared to the Ising model, there are fewer investigations for the three-dimensional *XY* and the Heisenberg model. In particular, to our knowledge, numerical determinations of the special transition and the corresponding surface critical exponents have not yet been reported for the *XY* model. Most of the existing results for the Ising, the *XY* and the Heisenberg model will be tabulated below, together with results of the present work.

The present work aims to provide an extensive and systematic Monte Carlo investigation of the phase transitions of the surfaces of the three-dimensional Ising, *XY*, and Heisenberg models. Compared to numerical investigations one or two decades ago, one has the following advantages. First, the bulk critical points of these systems have now been determined accurately. On the simple cubic lattice, the bulk critical point of the Ising model was determined as $K_c(n=1)=0.221\,654\,55$ (3) [24], with the uncertainty only in the eighth decimal place. The bulk transitions of the *XY* and the Heisenberg model were also determined [14,25–30] to occur at $K_c=0.454\,167$ (4) and 0.693 002 (12), respectively. In the present paper, we also simulate these two systems with periodic boundary conditions, and improve the above estimations as $K_c(n=2)=0.454\,1659$ (10) and $K_c(n=3)=0.693\,003$ (2). Second, the rapid development of computer technology makes it possible to perform extensive computations at a limited cost. The present work was performed on 20 personal computers (PCs); the total computer time is in the order of 20 CPU months at a processor speed of 2.5 GHz.

The organization of the present paper is as follows. Section II reviews the finite-size-scaling properties of the systems defined by Eq. (1), with the emphasis on the sampled quantities required for the numerical analysis of the simulation data. Section III describes the determination of the critical points of the *XY* and Heisenberg models. Sections IV, V, and VI present the Monte Carlo simulations and the results for the Ising, *XY*, and Heisenberg models, respectively. Section VII concludes the paper with a brief discussion.

II. FINITE-SIZE SCALING AND SAMPLED QUANTITIES

The total free energy of a system with free surfaces can, in analogy with the Hamiltonian in Eq. (1), be expressed as the sum of a bulk and a surface term [1,31,32]:

$$F = f_b V + f_1 S, \tag{2}$$

where f_b and f_1 are the densities of the bulk and the surface parts of the free energy, respectively, and V and S represent the total volume and the surface area, respectively. Near criticality, the finite-size scaling behavior of f_b and f_1 is given by the equations

$$f_b(t,h,L) = L^{-d} f_{bs}(tL^{y_t}, hL^{y_h}) + f_{ba}(t,h), \tag{3}$$

and

$$f_1(t,h,t_1,h_1,L) = L^{-(d-1)} f_{1s}(tL^{y_t}, hL^{y_h}, t_1 L^{y_{t1}}, h_1 L^{y_{h1}}) + f_{1a}(t,h,t_1,h_1). \tag{4}$$

The functions f_{bs} and f_{ba} are the singular and the analytical parts of f_b; f_{1s} and f_{1a} similarly apply to the surface free-energy density f_1. The bulk thermal and magnetic scaling fields are represented by t and h, and the surface scaling fields by t_1 and h_1. The associated exponents are labeled with corresponding subscripts. As implied by Eq. (3), the leading scaling behavior of the bulk does not depend on the presence of free surfaces, although physical quantities near the surfaces can be significantly affected.

On the basis of Eqs. (3) and (4), the scaling behavior of various quantities can be obtained as derivatives of f_b and f_1 with respect to the appropriate scaling fields. Details can be found in Ref. [1].

The determination of the bulk critical points used simulations of $L \times L \times L$ with periodic boundary conditions in which case f_1 vanishes. The sampling procedure involved the determination of the bulk magnetization density

$$\vec{m} \equiv N^{-1} \sum_{x,y,z=1}^{N} \vec{s}_{x,y,z}, \tag{5}$$

where $N = L^3$. This yielded the averages of the magnetization moments $\langle \vec{m} \cdot \vec{m} \rangle$ and $\langle (\vec{m} \cdot \vec{m})^2 \rangle$. The quantity

$$Q(K,L) \equiv \frac{\langle \vec{m} \cdot \vec{m} \rangle^2}{\langle (\vec{m} \cdot \vec{m})^2 \rangle}, \tag{6}$$

which is related to the Binder cumulant [33], converges to a universal value Q at the critical point, and was used to determine the critical coupling K_c. The finite-size scaling behavior of Q can be found by writing the moments of $\vec{m}$ in terms of derivatives of the free energy with respect to the magnetic field. After application of a scaling transformation, the singular powers in Q associated with field derivatives cancel, as do the powers of the nonuniversal metric factor relating the physical field and the magnetic scaling field. In the vicinity of the critical point one obtains, in terms of the temperature scaling field t and an irrelevant temperaturelike field u,

$$Q(t,u,L) = \tilde{Q}(tL^{y_t}, uL^{y_i}) + b_2 L^{3-2y_h} + b_3 L^{y_t - 2y_h} + \cdots, \tag{7}$$

where y_i is the leading irrelevant exponent. The correction term with amplitude b_2 is due to the analytic contribution to the second moment of $\vec{m}$, and that with amplitude b_3 to the second-order dependence of the temperature field on the physical magnetic field. Apart from corrections, the temperature field is proportional to $K - K_c$. Equation (7) will be used in Sec. III to determine the bulk critical points.

In order to investigate surface critical behavior, we simulated $L \times L \times L$ simple-cubic lattices with periodic boundary conditions in the xy plane and free boundaries in the z direction. First, we sampled the components of the surface magnetization and obtained two generalized surface susceptibilities

$$\chi_{11} = \frac{L^2}{2} \langle \vec{m}_1 \cdot \vec{m}_1 + \vec{m}_2 \cdot \vec{m}_2 \rangle, \text{ and } \chi_{12} = L^2 \langle \vec{m}_1 \cdot \vec{m}_2 \rangle, \tag{8}$$

where $\vec{m}_1$ and $\vec{m}_2$ are the magnetization densities at the free surfaces with $z=1$ and $z=L$, respectively. By differentiating the surface free energy with respect to magnetic fields that act on either one of the free surfaces, one finds that the singular parts of these surface susceptibilities scale as $L^{2y_{h1}-2}$.

In addition, we computed two surface-surface correlations. To define these, we explicitly label the spins by their Cartesian coordinates

$$g_{11} = \frac{1}{2L^2} \sum_{x,y=1}^{L} (\langle \vec{s}_{x,y,1} \cdot \vec{s}_{x+r,y+r,1} + \vec{s}_{x,y,L} \cdot \vec{s}_{x+r,y+r,L} \rangle) \quad (r = L/2), \tag{9}$$

and

$$g_{12} = \frac{1}{L^2} \sum_{x,y=1}^{L} \langle \vec{s}_{x,y,1} \cdot \vec{s}_{x,y,L} \rangle. \tag{10}$$

Further, we sampled two ratios of surface magnetization moments

$$Q_{11} = \frac{\langle \vec{m}_1 \cdot \vec{m}_1 \rangle^2}{\langle (\vec{m}_1 \cdot \vec{m}_1)^2 \rangle} \text{ and } Q_{12} = \frac{\langle \vec{m}_1 \cdot \vec{m}_2 \rangle^2}{\langle (\vec{m}_1 \cdot \vec{m}_2)^2 \rangle}. \tag{11}$$

These quantities are the surface analogs of the bulk ratio Q, cf. Eq. (7), and will be used to locate the surface transitions.

III. CRITICAL POINTS OF THE O(2) AND THE O(3) MODELS

The critical point of the Ising model on the simple cubic lattice is already known [24] with sufficient accuracy for the present purposes. We therefore restrict ourselves to the XY and Heisenberg models. We used a version of the Wolff cluster algorithm [34,35] to simulate these models in a zero field, on simple-cubic lattices with periodic boundary conditions. The Cartesian components, s^x, s^y, and s^z, of the spin vectors are stored in computer memory; they satisfy $(s^x)^2 + (s^y)^2 + (s^z)^2 = 1$, where $s^z = 0$ for the XY model. Each cluster is constructed on the basis of the Cartesian component s^y, which can be inverted by the Monte Carlo algorithm. In this sense, the spin components are treated as Ising spins. Each simulation consists of a large number of cycles, each of which contains several Wolff steps and a data sampling procedure. The cluster flips do not change the absolute values of the spin components. Thus, to satisfy ergodicity, each cycle also includes a random rotation of the whole system of spin

TABLE I. Description of the simulations of the *XY* and Heisenberg models. The table lists the simulation length in millions of cycles (#MC) as defined in Sec. III, and the number of Wolff clusters (#Wc/C) per cycle, for each system size L. The data for $L=8$, 16, and 32 were taken for several values of K in a range ΔK about the critical point K_c. The values shown are those for the *XY* model; those for the Heisenberg model are approximately the same.

L	#MC	#Wc/C	ΔK
4	50	2	0
6	50	3	0
8	50	4	0.012
10	20	5	0
12	20	6	0
14	20	7	0
16	80	8	0.004
20	20	10	0
24	20	12	0
28	20	14	0
32	80	16	0.0012
40	20	20	0
48	20	24	0
64	20	32	0
96	15	48	0
160	6.7	80	0

vectors. For the purpose of sampling the canonical ensemble, the net result is the same as the application of the Wolff algorithm in a randomly chosen direction. We simulated a number of L^3 systems whose finite sizes L are listed in Table I, together with the number of Wolff clusters per cycle and the total number of cycles per system size.

Most simulations of the *XY* model took place at $K=0.454\,15$, and of the Heisenberg model at $K=0.693$. Both values are already very close to the final estimates that we shall report for the respective critical points. To avoid bias effects associated with short binary shift registers [36,37] we took two such shift registers, with lengths equal to the Mersenne exponents 127 and 9689, and added the resulting two maximum-length bit sequences modulo 2. This procedure leads to a sequence whose leading deviation from randomness is a nine-bit correlation, which is a considerable improvement in comparison with the usual three-bit correlations [38].

The simulations yielded data for the Binder cumulant as described in the preceding Section. Its finite-size scaling behavior is found by expanding $\tilde{Q}$ in Eq. (7) and expressing the temperature deviation from the critical point in $K-K_c$:

$$Q(K,L) = Q + a_1(K-K_c)L^{y_t} + a_2(K-K_c)^2L^{2y_t} + \cdots + b_1L^{y_i} + b_2L^{3-2y_h} + b_3L^{y_t-2y_h} + \cdots, \quad (12)$$

where Q is a universal constant and the correction term with amplitude b_1 is due to the irrelevant field. This expression was used to analyze the numerical data for $Q(K,L)$ by means of least-squares fits. The exponents were set to the estimates obtained by Guida and Zinn-Justin [39], namely, $y_t=1.492$, $y_i=-0.789$, and $y_h=2.482$ for the *XY* model, and $y_t=1.414$, $y_i=-0.782$, and $y_h=2.482$ for the Heisenberg model. In order to determine the amplitudes a_1 and a_2 we included some data for relatively small ($L=8$, 16, and 32) systems, taken at values of K differing up to the order of 1% from K_c.

For the convenience of the reader, we summarize a few salient points of the multivariate analysis as applied here to the Binder ratio. In order to obtain satisfactory fits, as judged by the residual χ^2 per degree of freedom, systems with sizes smaller than a threshold value $L_{\min}$ were discarded. Naturally, $L_{\min}$ depends on the number of finite-size corrections, i.e., the terms with amplitudes b_1, b_2, … included in the fits. Including three such correction terms, satisfactory fits were obtained including all system sizes down to $L_{\min}=4$. We have also included mixed terms proportional to $(K-K_c)L^{y_i+y_t}$; these terms were found to be insignificant. Furthermore, we varied the number of temperature-dependent terms in Eq. (12), i.e., those with amplitudes a_1, a_2, … . Including three such terms, the data for all temperature ranges specified in Table I could be accommodated. Satisfactory fits with two such terms could be obtained after narrowing down the temperature range to about one half of the original one. The behavior of some relevant quantities in these fits, such as the residual χ^2 and the K_c estimate and its error, is illustrated in Table II for a small subset of the fits actually made.

The final estimates of the critical points and their uncertainty margins are based on the individual results of many different fits and on their mutual consistency. In other words, the effect of variation of the fitting procedure is included in the final error estimates. We have checked that the uncertainty in the exponents in the fit formula does not significantly increase the estimated errors. The results for the critical points are $K_c=0.454\,1659$ (10) for the *XY* model and $K_c=0.693\,003$ (2) for the Heisenberg model. The universal values of the amplitude ratios are $Q=0.8050$ (2) for the *XY* model and $Q=0.8776$ (2) for the Heisenberg model. The present results and some recent values taken from the literature are summarized in Table III.

IV. ISING MODEL

Although the three-dimensional Ising model has not been exactly solved, considerable information about its critical behavior is available from extensive investigations using various kinds of approximations. For a review see, e.g., Ref. [45]. For instance, evidence has been found that the Ising model is conformally invariant in three dimensions [23,46]. There is some consensus that the values of the bulk thermal and magnetic exponents, y_t and y_h, are 1.587 and 2.482, respectively, with uncertainty only in the last decimal place. The bulk critical points of a variety of three-dimensional systems with Ising universality have also been obtained [24]; the bulk transition of the Ising model with nearest-neighbor interactions on the simple-cubic lattice was determined as $K_c=0.221\,654\,55$ (3). The present work conveniently chooses this model so that no further work to determine K_c is required. As mentioned earlier, periodic boundary conditions are imposed in the xy plane and free boundaries along the z direction.

TABLE II. Some data for typical fits of the Binder cumulant of the *XY* and Heisenberg models. Only data for system sizes $L \geq L_{\min}$ were included in the fits. The exponents in the fit formula Eq. (12) were fixed at values taken from the literature. The parameters K_c, Q, a_1, a_2, a_3, and b_1 were fitted. In fits with $n_{\rm par}=7$ or more parameters, b_2 was also fitted, and fits with 8 parameters also included b_3. The following columns show the residual χ^2, the number of degrees of freedom, and the estimated critical point, and its statistical error.

Model	$L_{\min}$	$n_{\rm par}$	χ^2	d_f	K_c	
O(2)	10	6	19	26	0.454 1667	(5)
O(2)	14	6	9	22	0.454 1664	(5)
O(2)	20	6	7	14	0.454 1662	(6)
O(2)	6	7	22	35	0.454 1656	(5)
O(2)	8	7	19	33	0.454 1658	(6)
O(2)	10	7	14	25	0.454 1658	(6)
O(2)	4	8	21	36	0.454 1661	(5)
O(2)	6	8	21	34	0.454 1660	(6)
O(2)	8	8	19	32	0.454 1659	(8)
O(3)	6	6	63	41	0.692 9993	(10)
O(3)	8	6	42	39	0.693 0009	(10)
O(3)	10	6	28	31	0.693 0021	(11)
O(3)	6	7	37	40	0.693 0031	(12)
O(3)	8	7	35	38	0.693 0032	(14)
O(3)	10	7	28	30	0.693 0026	(15)
O(3)	4	8	41	41	0.693 0040	(13)
O(3)	6	8	37	39	0.693 0033	(15)
O(3)	8	8	35	37	0.693 0032	(19)

A. Ordinary phase transition

Using the Wolff cluster algorithm [34,35], we simulated the Ising model at bulk criticality, with the surface couplings chosen equal to the bulk couplings, i.e., $K_1=K=K_c$. The system sizes were taken as 16 even values in the range $4 \leqslant L \leqslant 48$. During the Monte Carlo simulations, we sampled the surface susceptibilities χ_{11} and χ_{12}, and the correlation functions g_{11} and g_{12}. To estimate $y_{h1}^{(o)}$, the universal surface magnetic exponent of the ordinary surface transition, we modeled the Monte Carlo data for the surface susceptibilities χ_{11} and χ_{12} by expressions of the form

$$\chi_1(L) = \chi_a + L^{2y_{h1}^{(o)}-2}(b_0 + b_1 L^{y_i} + b_2 L^{y_{t1}^{(o)}} + b_3 L^{y_3} + b_4 L^{y_4}), \tag{13}$$

where χ_a and the b_i are nonuniversal and depend on the characteristics of the surface; χ_1 stands for either one of χ_{11} and χ_{12}. The various parameters in this expression were determined by a least-squares fit. We set $\chi_a=0$ to fit χ_{12}.

Similarly, we fitted data for the correlation functions g_{11} and g_{12} to expressions of the form

$$g_1(L) = L^{2y_{h1}^{(o)}-4}[b_0 + b_1 L^{y_i} + b_2 L^{y_{t1}^{(o)}} + b_3 L^{y_3} + b_4 L^{y_4}], \tag{14}$$

Again, g_1 can be either g_{11} or g_{12}; the nonuniversal amplitudes b_i are fitting parameters independent of the corresponding amplitudes in Eq. (13), although we use the same symbols.

TABLE III. Summary of recent results for the critical coupling K_c of the three-dimensional *XY* and Heisenberg models on the simple-cubic lattice with nearest-neighbor interactions. The error margin in the last decimal place is shown in parentheses.

Reference	Model	Year	K_c	
[40]	O(2)	1993	0.454 08	(8)
[28]	O(2)	1993	0.454 14	(7)
[41]	O(2)	1993	0.454 20	(2)
[42]	O(2)	1997	0.454 19	(3)
[30]	O(2)	1996	0.454 165	(4)
[29]	O(2)	2002	0.454 167	(4)
Present work	O(2)	2005	0.454 1659	(10)
[43]	O(3)	1993	0.693 035	(37)
[44]	O(3)	1993	0.6930	(1)
[42]	O(3)	1997	0.693 05	(4)
[30]	O(3)	1996	0.693 002	(12)
Present work	O(3)	2005	0.693 003	(2)

The correction terms with amplitudes b_1, b_2, b_3, and b_4 in Eqs. (13) and (14) account for the leading finite-size corrections. The exponent $y_i=-0.821$ (5) [24] is the leading irrelevant thermal scaling field in the three-dimensional Ising universality class. Further, since the thermal surface scaling field for the ordinary transition is irrelevant, it may also introduce finite-size corrections. From a simple scaling argument it can be derived that the value of this irrelevant surface exponent is $y_{t1}^{(o)}=-1$ [47], independent of the spatial dimensionality. In principle, finite-size corrections from other sources can occur, so that we also include the terms with amplitudes b_3 and b_4. We simply took $y_3=-2$ and $y_4=-3$.

Separate fits of the χ_{11} and χ_{12} data, employing Eq. (13), yield consistent estimates: $y_{h1}^{(o)}=0.736$ (2) and 0.738 (2), respectively.

Fits of g_{11} and g_{12} yield $y_{h1}^{(o)}=0.737$ (2) and 0.736 (2), respectively. A joint fit of both sets of susceptibility data, as well as one of both sets of correlation function data, employing a single parameter $y_{h1}^{(o)}$ and independently variable amplitudes, yielded consistent results but no significant improvement of the accuracy.

We also simulated Ising systems in which the surface enhancement is defined as in Ref. [5]. These systems differ from Eq. (1) as to the couplings between the surface layer and the second layer. We thus introduce an enhancement parameter ϵ and define couplings $K_1=\epsilon^2 K$ between nearest-neighbor sites on the surface, and couplings $K_1'=\epsilon K$ between surface sites and their nearest neighbors in next layer. Using Cartesian coordinates to label the spins, the latter couplings between layers 1 and 2 are thus of the form $-K_1' s_{x,y,1} s_{x,y,2}$, instead of $-K s_{x,y,1} s_{x,y,2}$ as implied by Eq. (Ham1), and similarly for layers $L-1$ and L. Whenever we parametrize the surface enhancement by ϵ we refer to the Hamiltonian defined in Ref. [5], which differs from Eq. (1).

By varying the parameter ϵ, one can move closer to the fixed point for the ordinary phase transition so as to reduce

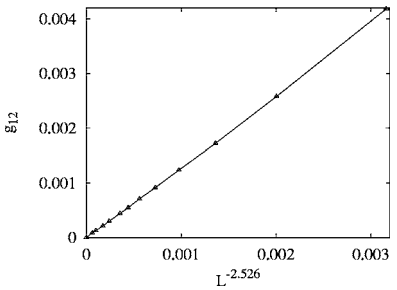

FIG. 2. Surface correlation function g_{12} vs $L^{-2.526}$ for the Ising model with $\epsilon=0.8$. For the purpose of visualization, the data points are connected by straight lines, in this as well as in the following figures. The error margins are of the same order as the thickness of the lines.

the amplitudes of finite-size corrections. Systems with $\epsilon=1$ reduce to those described above. In accordance with Ref. [5], in the present work we also chose $\epsilon=0.9$ and 0.8. The analyses of the data for the surface susceptibilities and the correlation functions again employ Eqs. (13) and (14); the results for the surface magnetic exponents are in agreement with those obtained for the case $\epsilon=1$. As an illustration, the data for g_{12} with $\epsilon=0.8$ are shown vs $L^{2y_{h1}^{(o)}-4}$ in Fig. 2, where $y_{h1}^{(o)}=0.737$ is taken from the fit.

Finally, a joint fit to the data for χ_{11} and χ_{12} for the three cases $\epsilon=1.0$, 0.9, and 0.8 yields $y_{h1}^{(o)}=0.7374$ (15); this result is in good agreement with most of the existing results, as shown in Table IV.

B. Special phase transition

Since it is known that the special transition is located near $\kappa=(K_1/K)-1=0.5$, the simulations were performed with surface enhancements κ in the range from 0.46 to 0.54, in steps of 0.01. The system sizes assumed 18 values in the range $5 \leqslant L \leqslant 95$. We sampled several quantities, including the surface susceptibilities χ_{11} and χ_{12}, and the universal ratios Q_{11} and Q_{12}. Part of the data for Q_{11} are shown in Fig. 3, in which the clear intersection indicates the location $\kappa_c^{(s)}$ of the special transition. As mentioned earlier, when κ deviates from $\kappa_c^{(s)}$, the finite-size behavior of Q_{11} is governed by the surface thermal exponent $y_{t1}^{(s)}$. We fitted the data for Q_{11} and Q_{12} by

$$
\begin{aligned}
Q_1(\kappa,L) = Q_{1c}^{(s)} + \sum_{k=1}^{4} a_k[\kappa-\kappa_c^{(s)}]^k L^{ky_{t1}^{(s)}} + \sum_{l=1}^{4} b_l L^{y_l} \\
+ c[\kappa-\kappa_c^{(s)}]L^{y_{t1}^{(s)}+y_i} + n[\kappa-\kappa_c^{(s)}]^2 L^{y_{t1}^{(s)}} + r_0 L^{y_a} \\
+ r_1[\kappa-\kappa_c^{(s)}]L^{y_a} + r_2[\kappa-\kappa_c^{(s)}]^2 L^{y_a} \\
+ r_3[\kappa-\kappa_c^{(s)}]^3 L^{y_a},
\end{aligned}
\tag{15}
$$

where the terms with amplitude b_l account for various finite-size corrections; and again the subindex 1 in Q_1 and Q_{1c} is shorthand for 11 or 12, whichever the case may be. The terms with amplitudes r_i ($i=0, \ldots, 3$) are due to the analytic background. The derivation of Eq. (15) can be found, e.g., in Ref. [24]. Naturally, we fixed the exponent $y_1=y_i=-0.821$ (5) [24], the exponent of the leading irrelevant scaling field in the three-dimensional Ising model. In principle, additional

TABLE IV. Summary of the results for the surface critical exponents in the three-dimensional Ising model, as obtained by different techniques. MF: mean-field theory, MC: Monte Carlo simulations, FT: field-theoretical methods, CI: conformal invariance. The MF values of y_{t1} and y_{h1} have already made use of the mean-field predictions for the bulk thermal and magnetic exponents, which are $y_t=3/2$ and $y_h=9/4$, respectively.

	Ordinary		Special			
	y_{h1}	β_1	y_{h1}	y_{t1}	β_1	ϕ
MF[a]	1/2	1	5/4	3/4	1/2	1/2
MC[b]	0.72 (3)	0.78 (2)	1.71 (16)	0.94 (5)	0.18 (2)	0.59 (4)
MC[c]	0.721 (6)	0.807 (4)	1.623 (3)		0.2375 (15)	
MC[d]	0.740 (15)					
MC[e]	0.73 (1)	0.80 (1)				
MC+CI[f]	0.737 (5)	0.798 (5)				
MC[g]			1.624 (8)	0.73 (2)	0.237 (5)	0.461 (15)
FT[h]	0.737	0.796	1.583	0.855	0.263	0.539
FT[i]	0.706	0.816				
FT[j]			1.611	1.08	0.245	0.68
Present	0.7374 (15)	0.796 (1)	1.636 (1)	0.715 (1)	0.229 (1)	0.451 (1)

[a]See Refs. [1,11].
[b]See Ref. [18].
[c]See Ref. [20].
[d]See Ref. [5].
[e]See Ref. [21].
[f]See Ref. [23].
[g]See Ref. [19].
[h]See Ref. [2,15].
[i]See Ref. [16].
[j]See Ref. [17].

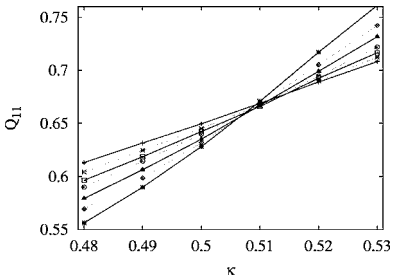

FIG. 3. Surface dimensionless ratio Q_{11} vs surface-coupling enhancement κ for the Ising model. The data points +, ×, □, ○, △, ◇, and * represent system sizes $L=21$, 25, 29, 33, 41, 49, and 63, respectively.

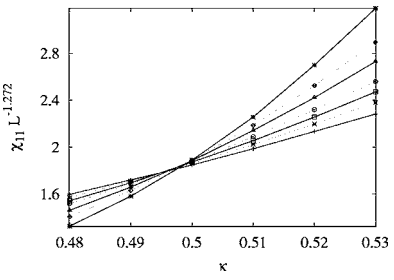

FIG. 4. Surface susceptibility $\chi_{11}L^{-1.272}$ vs surface-coupling enhancement κ for the Ising model. The data points +, ×, □, ○, △, ◇, and * represent system sizes $L=21$, 25, 29, 33, 41, 49, and 63, respectively.

corrections due to irrelevant scaling fields can be induced by the open surfaces, so that we set $y_2=y_{i1}$ as an unknown exponent. In order to reduce the residual χ^2 without discarding data for many small system sizes, we included further finite-size corrections with integer powers $y_3=-2$ and $y_4=-3$. The term with coefficient n reflects the nonlinear dependence of the scaling field on κ, and the one with c describes the "mixed" effect of the surface thermal field and the irrelevant field. The terms with amplitudes r_0, r_1, r_2, and r_3 arise from the analytical part of the free energy, and the exponent y_a is equal to $2-2y_{h1}^{(s)}$. As determined later, the surface magnetic exponent at the special transition is about $y_{h1}^{(s)}=1.636$ (1), so that we fixed the exponent $y_a=-1.272$. The fits of Q_{11} yields $Q_{11c}=0.626$ (1), $\kappa_c^{(s)}=0.502\,14$ (8), and $y_{t1}^{(s)}=0.7154$ (14); from the fit of Q_{12}, we obtain $Q_{12c}=0.2689$ (1), $\kappa_c^{(s)}=0.502\,07$ (8), and $y_{t1}^{(s)}=0.715$ (4). Next, we simultaneously fitted the data for Q_{11} and Q_{12} by Eq. (15), and obtain $\kappa_c^{(s)}=0.502\,08$ (5), and $y_{t1}^{(s)}=0.715$ (1). Our estimate $\kappa_c^{(s)}=0.502\,08$ (5) does not agree well with the existing results $\kappa_c^{(s)}=0.5004$ (2) [19,20]. Further, as expected, $\kappa_c^{(s)}$ does not assume the mean-field value 1/2. Attempts to determine the unknown exponent y_{i1} and its associated amplitude by least-square fitting to the Q_{11} and Q_{12} data were unsuccessful. These corrections, if present, do not exceed the detection threshold. We also fitted the data for the surface susceptibilities χ_{11} and χ_{12} by

$$\chi_1(\kappa,L) = L^{2y_{h1}^{(s)}-2}\Bigg\{ a_0 + \sum_{k=1}^{4} a_k[\kappa-\kappa_c^{(s)}]^k L^{ky_{t1}^{(s)}} + b_1 L^{y_i} + b_2 L^{y_{i1}} + b_3 L^{y_3} + b_4 L^{y_4} + c[\kappa-\kappa_c^{(s)}]L^{y_{t1}^{(s)}+y_i} + n[\kappa-\kappa_c^{(s)}]^2 L^{y_{t1}^{(s)}} + r_0 L^{y_a} + r_1[\kappa-\kappa_c^{(s)}]L^{y_a} + r_2[\kappa-\kappa_c^{(s)}]^2 L^{y_a} + r_3[\kappa-\kappa_c^{(s)}]^3 L^{y_a} + c_{21}[\kappa-\kappa_c^{(s)}]L^{y_{t1}^{(s)}+y_{i1}} + c_{22}[\kappa-\kappa_c^{(s)}]^2 L^{2y_{t1}^{(s)}+y_{i1}} \Bigg\}. \tag{16}$$

Again, the correction exponents were taken as $y_i=-0.821$ (5) [24], $y_3=-2$, and $y_4=-3$, and the exponent $y_2=y_{i1}$ was left to be fitted. Other than in Eq. (15), we have included in Eq. (16) the combined effect of the surface thermal field and the irrelevant field with the unknown exponent y_{i1}, as described by the mixed terms with amplitudes c_{21} and c_{22}. These terms lead to a reduction of the residual χ^2 of the fits, but do not significantly modify the result for the surface exponent $y_{h1}^{(s)}$. The surface thermal exponent was fixed at $y_{t1}^{(s)}=0.715$ as found above. The fit of χ_{11} yields $\kappa_c^{(s)}=0.502\,09$ (9), $y_{h1}^{(s)}=1.636$ (1), and $y_{i1}=-0.52$ (2). The quoted error margins include the uncertainty due to the error in $y_{t1}^{(s)}$. In this case we found clear evidence for corrections, introduced by the surfaces with an exponent y_{i1}. It is remarkable that such corrections are significant only in combination with κ-dependent terms. The data for the surface susceptibility are shown in Fig. 4 as $\chi_1(\kappa,L)L^{-1.272}$, where the exponent, which stands for $2-2y_{h1}^{(s)}$, is chosen such as to suppress the leading L dependence at the special transition. As expected, the data display intersections approaching the special transition as determined above.

V. *XY* MODEL

The bulk critical point of the *XY* model was determined as $K_c=0.454\,1659$ (10) in Sec. II. The following simulations were performed at $K=0.454\,166$. The results in this section do not significantly depend on the possible difference of about 10^{-6} with the actual critical point.

A. Ordinary phase transition

In analogy with the Ising model, we first let the surface couplings K_1 assume the same values of the bulk couplings, i.e., $K_1=K=K_c$. The system size took 14 values in the range $4\leqslant L\leqslant 48$. We sampled the surface susceptibilities χ_{11} and χ_{12}, and the correlation functions g_{11} and g_{12}, and analyzed the data as we did for the Ising model at the ordinary phase transition. For instance, the data for χ_{11} and χ_{12} were also fitted by Eq. (13), in which the irrelevant exponent was taken as $y_i=-0.789$ [39]. The estimates of the surface magnetic exponent $y_{h1}^{(o)}$ from various quantities agree; the result is $y_{h1}^{(o)}=0.781$ (2).

As a consistency test, in analogy with the Ising model, we also simulated the surface-enhanced *XY* model as defined in Ref. [5], with $\epsilon=0.9$ and 0.8. As expected, the results for these two cases are in good agreement with the above estimate $y_{h1}^{(o)}=0.781$ (2). However, since the simulations are less

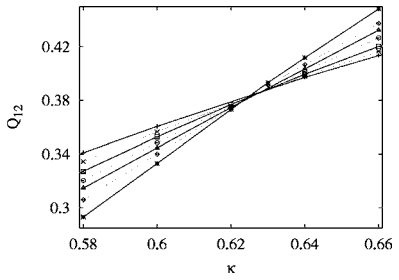

FIG. 5. Surface dimensionless ratio Q_{12} vs surface-coupling enhancement κ for the XY model. The data points +, ×, □, ○, △, ◇, and * represent system sizes $L=17$, 21, 25, 33, 41, 49, and 63, respectively.

extensive in comparison with those for the case $\epsilon=1$, they do not significantly improve the accuracy of $y_{h1}^{(o)}$.

B. Special phase transition

As discussed above, the XY model is a marginal case in the sense that the line of surface phase transitions for $K<K_c$ is Kosterlitz-Thouless-like. Still, one would expect that, for $K=K_c$, the special and the extraordinary surface transitions occur. Therefore, we performed simulations at the estimated bulk critical point as given above, and varied the surface enhancement from $\kappa=0.48$ to $\kappa=0.68$. The system sizes took on 19 values in the range $5\leqslant L\leqslant 95$. The sampled quantities include the surface susceptibilities χ_{11} and χ_{12}, the correlation functions g_{11} and g_{12}, and the dimensionless ratios Q_{11} and Q_{12}. Part of the data for Q_{12} are shown in Fig. 5, where the intersection clearly indicates that the special transition occurs near $\kappa_c=0.622$. Further, the increase of the slope of Q as a function of finite size L strongly suggests that the surface thermal exponent at κ_c is larger than 0, i.e., that the scaling field associated with κ is not marginal at the special transition. The data for Q_{11} and Q_{12} were fitted by Eq. (15), in which the leading irrelevant exponent was fixed at $y_i=-0.789$ [39] and the exponent $y_2=y_{i1}$ was left free. We obtain $Q_{11c}=0.840$ (1), $Q_{12c}=0.379$ (2), $\kappa_c=0.6222$ (3), and $y_{t1}^{(s)}=0.608$ (4). The fits of Q_{11} and Q_{12} do not provide clear evidence for the existence of a term with exponent y_{i1}.

We also fitted the surface susceptibilities χ_{11} and χ_{12} by Eq. (16). We obtain the surface magnetic exponent as $y_{h1}^{(s)}=1.675$ (1). Further, we find evidence for new finite-size-corrections with exponent $y_{i1}=-0.44$ (4), the major contribution to which comes from the mixed terms with amplitudes c_{21} and c_{22} in Eq. (16). Results for the surface exponents are summarized in Table V.

TABLE V. Summary of the results for the surface critical exponents in the three-dimensional XY and Heisenberg models. MC: Monte Carlo simulations, SE: series expansions.

	Ordinary	Special	
	y_{h1}	y_{h1}	y_{t1}
MC (XY)[a]	0.74		
SE (XY)[b]	0.81		
MC (XY)[c]	0.790 (15)		
Present(XY)	0.781 (2)	1.675 (1)	0.608 (4)
MC (Heisenberg)[c]	0.79 (2)		
Present (Heisenberg)	0.813 (2)		

[a]See Ref. [7].
[b]See Ref [14].
[c]See Ref. [5].

C. Extraordinary phase transition

Two-dimensional surfaces of the XY model do not display spontaneous long-ranged surface order for $K<K_c$, but they are in a ferromagnetic state in the low-temperature region $K>K_c$. Thus the onset of long-range order on the surface also occurs at $K=K_c$. This differs from the Ising model, where a long-range ordered surface exists for $K<K_c$ if $\kappa>\kappa_c$. We performed simulations at $\kappa=1$ for the critical XY model with the system sizes in the range $7\leqslant L\leqslant 95$. We sampled the second moment of the surface magnetization m_1^2 and the ratio Q_{11}; the data for these two quantities are shown in Table VI.

In order to analyze the finite-size data in Table VI, one first requires the proper scaling formulas. For the extraordinary phase transitions in the XY model, there exists some ambiguity, because it is not generally clear whether the surfaces undergo a first or a second order transition. Nevertheless, in either case, the surfaces should display some critical singularities, arising from the diverging bulk correlation length. Thus, we fitted the m_1^2 data by

$$m_1^2(L) = m_a^2 + L^{-2X_{h1}^{(e)}}(b_0 + b_1 L^{y_1} + b_2 L^{2y_1}). \qquad (17)$$

If the transition on the surface is first order at $K=K_c$, the analytical contribution, m_a^2, assumes a nonzero value. First,

TABLE VI. Monte Carlo data for the second moment of surface magnetization m_1^2 and the dimensionless ratio Q_{11} for the three-dimensional XY model with enhancement $\kappa=1$.

L	7	9	11	13	17	21	25
m_1^2	0.5653 (1)	0.5293 (1)	0.5037 (1)	0.4839 (1)	0.4561 (1)	0.4364 (1)	0.4216 (1)
Q_{11}	0.962 42 (6)	0.965 80 (6)	0.968 78 (5)	0.971 38 (4)	0.975 43 (3)	0.978 35 (3)	0.980 65 (3)
L	33	41	49	63	71	81	95
m_1^2	0.4004 (1)	0.3859 (1)	0.3747 (1)	0.3601 (1)	0.3540 (1)	0.3473 (1)	0.3397 (1)
Q_{11}	0.983 81 (3)	0.986 01 (3)	0.987 48 (3)	0.989 27 (3)	0.990 04 (3)	0.990 85 (3)	0.991 69 (3)

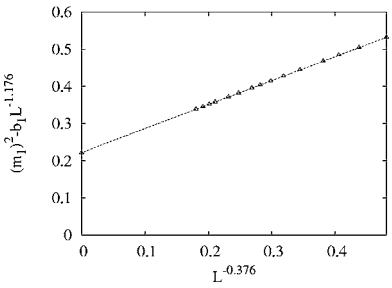

FIG. 6. Surface magnetization in terms of the quantity $(m_1)^2 - b_1 L^{-1.2}$ vs $L^{-2X_{h1}^{(e)}}$ for the XY model at $\kappa=1$, where the values $X_{h1}^{(e)}=0.188$ (5) and $b_1=0.35$ (5) were obtained from a least-squares fit (see text).

we set the exponent $y_1=y_i=-0.789$ [39]. Satisfactory fits were obtained for all the m_1^2 data in Table VI, with the terms m_a^2 and those with b_0 and b_1 only. The results are $m_a=0.471$ (5), $X_{h1}^{(e)}=0.188$ (5), $b_0=0.65$ (1), and $b_1=0.35$ (5). The quality of the fit is shown in Fig. 6. Further, we fitted the data for the ratio Q_{11} by

$$Q_{11}(L) = Q_c + b_1 L^{-2X_{h1}^{(e)}} + b_2 L^{-2X_{h1}^{(e)}+y_1} + b_3 L^{-2X_{h1}^{(e)}+2y_1} + b_4 L^{-2X_{h1}^{(e)}+3y_1}, \quad (18)$$

where the irrelevant exponent is fixed at $y_1=y_i=-0.789$ [39]. The presence of the exponent $X_{h1}^{(e)}$ is due to the nonzero background contribution m_a in the second moment of the magnetization m_1^2. We obtain the asymptotic value $Q_c=0.9998$ (4) ≈ 1. From the results for m_a and Q_c, it seems that the surface transition at $K=K_c$ and $\kappa=1$ is first order. However, it seems also possible that the surface magnetization vanishes only very slowly as the system size L increases, such that the line of extraordinary transitions on the surfaces is still Kosterlitz-Thouless-like. Thus, we set m_a in Eq. (17) to zero, and fitted the unknown parameters including both $X_{h1}^{(e)}$ and y_i to the m_1^2 data. Indeed, we found that our Monte Carlo data for m_1^2 in Table VI can be modeled this way, and we obtain $b_0=0.40$ (1), $b_1=0.703$ (6), $X_{h1}^{(e)}=0.0325$ (30), and $y_1=-0.545$ (14). This fit is illustrated by Fig. 7; the approximate linearity indicates the quality of the fit. We also fitted the Q data by Eq. (18) with y_1 fixed at -0.545, and the result for Q_c is $Q_c=0.9982$ (15), which is also consistent with 1. In short, our numerical evidence for the surface magnetization of the three-dimensional XY model is not sufficient to determine

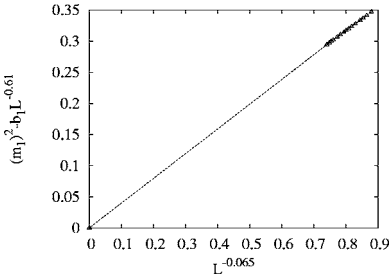

FIG. 7. Surface magnetization in terms of the quantity $(m_1)^2 - b_1 L^{-0.61}$ vs $L^{-0.065}$ for the XY model at $\kappa=1$.

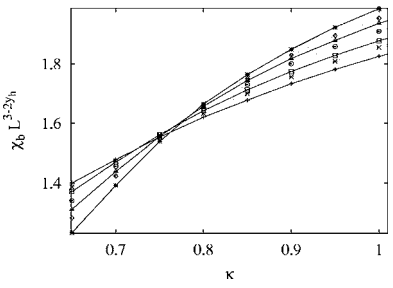

FIG. 8. Critical bulk susceptibility χ_b of the Heisenberg model vs. surface enhancement κ. The data shown along the vertical axis are scaled with a size-dependent factor L^{3-2y_h} where $y_h=2.482$ is the bulk magnetic exponent. The data points +, ×, □, ○, △, ◇, and * represent system sizes $L=16$, 20, 24, 32, 40, 48, and 64, respectively. According to the theory, the scaled susceptibility $\chi_b L^{3-2y_h}$ converges with increasing size L to a value that may still depend on κ. The intersections near $\kappa=0.8$ suggest the existence of a special phase transition.

whether the line of transitions for $K=K_c$ and $\kappa>\kappa_c$ is first or second order, but settling this matter convincingly would require extensive simulations, well beyond the scope of the present investigation.

VI. HEISENBERG MODEL

The bulk critical point of the three-dimensional Heisenberg model was determined as $K_c=0.693\,003$ (2) in Sec. II. The simulations reported in this section took place at at $K_1=K=K_c=0.693\,002$. We have checked that the possible difference of about 2×10^{-6} with the actual critical point affects the results in this section only in a very insignificant way.

The system sizes were taken in the range $4\leqslant L\leqslant 64$. The data for the surface susceptibilities χ_{11} and χ_{12}, taken at $\kappa=0$, were fitted by Eq. (13). Using a similar procedure as that for the XY model, we obtain $y_{h1}^{(o)}=0.813$ (2) for the ordinary phase transition. We also determined the bulk susceptibility χ_b and the dimensionless ratios Q_{11} and Q_{12} for a range of larger values of the surface enhancement κ. The scaled susceptibility $\chi_b L^{3-2y_h}$ is shown in Fig. 8. The intersections near $\kappa\approx 0.8$ are very suggestive of a special transition. The results for Q_{11}, shown in Figs. 9 and 10, display similar behavior. We mention that, because of finite-size corrections, it is natural that the intersection points between the data lines in Figs. 8 and 10 do not coincide. Nevertheless, for $L\to\infty$, the intersection points in both figures should converge to the same value of κ. For $\kappa\lesssim 0.8$, Q_{11} converges to a universal constant characteristic of the ordinary transition. For $\kappa\gtrsim 0.8$ the data seem to converge to a κ-dependent value. The overall behavior of the results for Q_{11} resembles that of the ratio Q for bulk transitions in the Kosterlitz–Thouless universality class, as reported for the triangular Ising antiferromagnet with nearest-neighbor and next-nearest-neighbor interactions [48]. An alternative interpretation would be a special transition with a relevant exponent $y_{t1}^{(s)}$ only slightly larger than 0. A convincing numerical test of the Kosterlitz–Thouless nature of the special transition would require simulations beyond the scope of the present work.

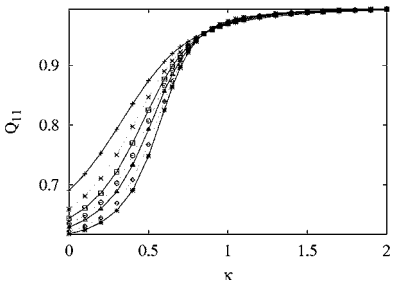

FIG. 9. Surface dimensionless ratio Q_{11} vs surface-coupling enhancement κ for the O(3) model. The data points +, ×, □, ○, △, ◇, and * represent system sizes $L=8$, 12, 16, 20, 24, 32, and 40, respectively. For small surface enhancement $\kappa \lesssim 0.5$, the ratio Q_{11} converges with increasing L to a nontrivial value near 0.62, just as expected for the ordinary phase transition. For large enhancement $\kappa > 1$, it seems that the asymptotic value $Q_{11}(L \to \infty)$ is different from 1, and dependent on κ. In the intermediate range $0.6 < \kappa < 0.9$, the slope of the Q_{11} data lines increases with L. The intersections of these lines seem to converge to a value near $\kappa = 0.8$. This figure bears much analogy with that for the bulk ratio Q of transitions in the Kosterlitz–Thouless universality class.

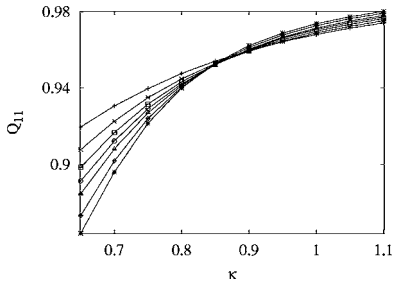

FIG. 10. Surface ratio Q_{11} in the range $0.65 \leqslant \kappa \leqslant 1.1$ for the O(3) model. The data points +, ×, □, ○, △, ◇, and * represent system sizes $L=8$, 16, 24, 32, 40, 48, and 64, respectively. The apparent convergence of the intersections of the Q_{11} data with increasing system size indicates a special surface transition near $\kappa = 0.80$, in agreement with the results in Figs. 8 and 9.

VII. DISCUSSION

We used Monte Carlo techniques and finite-size scaling in order to obtain more accurate results for the bulk and surface critical parameters of the three-dimensional Ising, *XY*, and Heisenberg models. At the ordinary phase transitions, we determined the surface magnetic exponents as $y_{h1}^{(o)}(n=1) = 0.7374$ (15), $y_{h1}^{(o)}(n=2) = 0.781$ (2), and $y_{h1}^{(o)}(n=3) = 0.813$ (2). These values are in a satisfactory agreement with earlier results [5], namely, $y_{h1}^{(o)}(n=1) = 0.740$ (15), $y_{h1}^{(o)}(n=2) = 0.790$ (15), and $y_{h1}^{(o)}(n=3) = 0.79$ (2), as shown in Table V. Since the bulk thermal exponent y_t of the O(n) model decreases with increasing n, these results suggest that the surface exponent $y_{h1}^{(o)}$ is a decreasing function of y_t. The same seems to hold true for the two-dimensional and three-dimensional Potts models, as may be concluded on the basis of the following evidence. In three dimensions, the surface magnetic exponent for the $q \to 0$ and $q \to 1$ Potts models are $y_{h1}^{(o)} = 2$ and 1.0246 (6) [50], respectively. The former model is generally referred to as the uniform spanning tree [49], while the $q \to 1$ Potts model reduces to the bond percolation model. For the two-dimensional Potts model, from the conformal field theory, the exponent $y_{h1}^{(o)}$ is exactly known as $y_{h1}^{(o)} = 2 - 3/(3 - y_t)$ [51], which is a decreasing function of the bulk thermal exponent y_t. Further, if one applies the above expression to the tricritical branch of the Potts model in two dimensions, one obtains that the surface magnetic scaling field is irrelevant at the ordinary phase transition. Starting from this observation, it was found [8] that rich surface phase transitions can also occur in some two-dimensional systems, although their "surfaces" are just one-dimensional edges.

In the present work, we also located the special transitions of the Ising and the *XY* model on the simple-cubic lattice, and obtained numerical estimates of the corresponding renormalization exponents. While the surface transition of the three-dimensional *XY* model is Kosterlitz-Thouless-like, and the line of surface transitions connects to the special transition point, our numerical data did not yield evidence for corrections to scaling due to a marginal field at the special transition.

Finally, we note that the surface-critical behavior of the O(1), O(2), and O(3) models is rather dissimilar for large surface enhancements. For the O(1) model, spontaneous surface order exists even below the bulk critical coupling K_c; for the O(2) model it exists for $K > K_c$ and possibly for $K = K_c$; and for the O(3) model only for $K > K_c$. In line with the bulk critical singularity, the O(n) surface critical behavior is thus seen to become less singular with increasing n. This is also evident from our analyses of the special transitions, which yield relevant exponents $y_{t1}^{(s)}$ for the O(1) and O(2) models but allow a marginal exponent for the O(3) model. Since the lower critical dimensionality of the special transition [1] is 3 for $n > 2$, it seems plausible that the range $\kappa > \kappa_c$ corresponds with a line of fixed points and κ-dependent critical surface exponents, in agreement with an analysis of the surface magnetization by Krech [9]. Indeed, the data in Figs. 8 and 9 are suggestive of a Kosterlitz-Thouless-like scenario involving a nonuniversal range of Q values such as found earlier in the different context of the Ising triangular antiferromagnet [48].

ACKNOWLEDGMENTS

The authors are indebted to Dr. J. R. Heringa and X. F. Qian for valuable discussions. This research was supported by the Dutch FOM foundation ("Stichting voor Fundamenteel Onderzoek der Materie") which is financially supported by the NWO ("Nederlandse Organisatie voor Wetenschappelijk Onderzoek"). This research was supported in part by the United States National Science Foundation under Grant No. ITR 0218858.

[1] K. Binder, in *Phase Transitions and Critical Phenomena*, edited by C. Domb and J. L. Lebowitz (Academic, London, 1987), Vol. 8, p. 1, and references therein.
[2] H. W. Diehl, in *Phase Transitions and Critical Phenomena*, edited by C. Domb and J. L. Lebowitz (Academic, London, 1987), Vol. 10, p. 76, and references therein.
[3] H. W. Diehl, Int. J. Mod. Phys. B **11**, 3503 (1997).
[4] M. Pleimling, J. Phys. A **37**, R79 (2004).
[5] M. P. Nightingale and H. W. J. Blöte, Phys. Rev. B **48**, 13 678 (1993).
[6] J. M. Kosterlitz and D. J. Thouless, J. Phys. C **5**, L124 (1973).
[7] D. P. Landau, R. Pandey, and K. Binder, Phys. Rev. B **39**, 12302 (1989).
[8] Y. Deng and H. W. J. Blöte, Phys. Rev. E **70**, 035107(R) (2004).
[9] M. Krech, Phys. Rev. B **62**, 6360 (2000).
[10] Y. Deng and H. W. J. Blöte (unpublished).
[11] K. Binder and P. C. Hohenberg, Phys. Rev. B **6**, 3461 (1972).
[12] K. Binder and P. C. Hohenberg, Phys. Rev. B **9**, 2194 (1974).
[13] T. C. Lubensky and M. H. Rubin, Phys. Rev. B **12**, 3885 (1975).
[14] K. Ohno, Y. Okabe, and A. Morita, Prog. Theor. Phys. **71**, 741 (1984).
[15] H. W. Diehl and M. Shpot, Nucl. Phys. B **528**, 595 (1998).
[16] H. W. Diehl and S. Dietrich, Z. Phys. B: Condens. Matter **42**, 65 (1981).
[17] H. W. Diehl and S. Dietrich, Phys. Rev. B **24**, 2878 (1981).
[18] D. P. Landau and K. Binder, Phys. Rev. B **41**, 4633 (1990).
[19] C. Ruge, A. Dunkelmann, F. Wagner, and J. Wulf, J. Stat. Phys. **73**, 293 (1993).
[20] C. Ruge and F. Wagner, Phys. Rev. B **52**, 4209 (1995).
[21] M. Pleimling and W. Selke, Eur. Phys. J. B **1**, 385 (1998).
[22] K. Binder, D. P. Landau, and M. Muller, J. Stat. Phys. **110**, 1411 (2003).
[23] Y. Deng and H. W. J. Blöte, Phys. Rev. E **67**, 066116 (2003).
[24] Y. Deng and H. W. J. Blöte, Phys. Rev. E **68**, 036125 (2003), and references therein.
[25] M. P. Nightingale, *Finite-Size Scaling and Numerical Simulation of Statistical Systems*, edited by V. Privman (World Scientific, Singapore, 1990), p. 287.
[26] M. P. Nightingale and H. W. J. Blöte, Phys. Rev. Lett. **60**, 1562 (1988).
[27] J. Adler, J. Phys. A **16**, 3585 (1983).
[28] J. Adler, C. Holm, and W. Janke, Physica A **201**, 581 (1993).
[29] A. Cucchieri, J. Engels, S. Holtmann, T. Mendes, and T. Schulze, J. Phys. A **35**, 6517 (2002).
[30] H. G. Ballesteros, L. A. Fernández, V. Martín-Mayor, and A. M. Sudupe, Phys. Lett. B **387**, 125 (1996).
[31] M. E. Fisher and G. Caginalp, Commun. Math. Phys. **56**, 11 (1977).
[32] G. Caginalp and M. E. Fisher, Commun. Math. Phys. **65**, 247 (1979).
[33] K. Binder, Z. Phys. B: Condens. Matter **43**, 119 (1981).
[34] U. Wolff, Phys. Rev. Lett. **62**, 361 (1989).
[35] U. Wolff, Phys. Lett. B **228**, 379 (1989).
[36] A. Hoogland, J. Spaa, B. Selman, and A. Compagner, J. Comput. Phys. **51**, 250 (1983).
[37] A. Hoogland, A. Compagner, and H. W. J. Blöte, in *Architecture and Performance of Specialized Computers*, in the series Computational Techniques, edited by B. Alder (Academic, New York, 1988) pp. 233.
[38] L. N. Shchur and H. W. J. Blöte, Phys. Rev. E **55**, R4905 (1997).
[39] R. Guida and J. Zinn-Justin, J. Phys. A **31**, 8103 (1998).
[40] W. Janke, Phys. Lett. A **148**, 306 (1990).
[41] A. P. Gottlob and M. Hasenbusch, Physica A **201**, 593 (1993).
[42] P. Butera and M. Comi, Phys. Rev. B **56**, 8212 (1997).
[43] K. Chen, A. M. Ferrenberg, and D. P. Landau, Phys. Rev. B **48**, 3249 (1993).
[44] C. Holm and W. Janke, Phys. Lett. A **173**, 8 (1993); Phys. Rev. B **48**, 936 (1993). This work has yielded a second estimate of K_c that is slightly smaller.
[45] K. Binder and E. Luijten, Phys. Rep. **344**, 179 (2001).
[46] Y. Deng and H. W. J. Blöte, Phys. Rev. Lett. **88**, 190602 (2002).
[47] T. W. Burkhardt and J. L. Cardy, J. Phys. A **20**, L233 (1987).
[48] X. F. Qian and H. W. J. Blöte, Phys. Rev. E **70**, 036112 (2004).
[49] For a review, see e.g., F. Y. Wu, Rev. Mod. Phys. **54**, 235 (1982).
[50] Y. Deng and H. W. J. Blöte, Phys. Rev. E **71**, 016117 (2005).
[51] J. L. Cardy, Nucl. Phys. B **240**, 514 (1984); **324**, 581 (1989).